

# Adsorption Kinetics of Hydrogen Sulfide and Thiols on GaAs (001) Surfaces in a Vacuum

Oleksandr Voznyy and Jan J. Dubowski\*

Department of Electrical and Computer Engineering, Centre d'Excellence en Genie de l'Information, Université de Sherbrooke, Sherbrooke, Québec J1K 2R1, Canada

Received: July 27, 2007; In Final Form: December 18, 2007

Adsorption mechanisms of hydrogen sulfide and alkanethiols on GaAs (001) surfaces prepared in a vacuum were studied using first principles calculations. The need for a physisorbed precursor was confirmed based on energetic arguments and molecular dynamics simulations of the transition from a physisorption to a chemisorption state. The preference for S–Ga bond formation was found, resulting from a weak non-dissociative chemisorption state formed by the overlap of a sulfur lone pair orbital with an empty Ga dangling bond. Physisorption energies and the height of the transition barrier from physisorption to chemisorption on GaAs were found to be very similar to those on gold, while the main difference from gold was that hydrogen remains on the GaAs surface upon S–H cleavage. Obtained results allowed for a more advanced interpretation of experimental data concerning H<sub>2</sub>S and thiol adsorption on GaAs.

## 1. Introduction

Formation of self-assembled monolayers (SAMs) of alkanethiols on III–V semiconductor surfaces has become an important task in recent years for prospective applications in surface passivation,<sup>1,2</sup> chemical and bio-sensing,<sup>3–5</sup> and hybrid molecule–semiconductor devices.<sup>6</sup> Thiol deposition on GaAs surfaces is possible from both vapor<sup>7–9</sup> and liquid<sup>10–14</sup> phases. However, SAM formation was investigated only for liquid-phase deposition. The growth of high-quality SAMs on GaAs is complicated and difficult to reproduce, as evidenced by the variation among different studies using nominally the same preparation procedures.<sup>10–14</sup> Moreover, available experimental data indicate a much slower SAM growth rate on GaAs as compared to that observed with gold.<sup>11,12</sup> Indeed, the process of thiol SAM formation on GaAs is more complex and diverse and is not as well-understood as that on gold.<sup>15,16</sup> A detailed investigation of thiol adsorption mechanisms is essential for understanding SAM growth kinetics and the improvement of thiol deposition techniques.

Experimental results indicate that the adsorption of thiols on gold proceeds via a physisorbed precursor.<sup>15,16</sup> Similar behavior is expected for thiols on GaAs. However, to our knowledge, the physisorption state of alkanethiols on GaAs has not been studied to date. In fact, even for the extensively studied adsorption of thiols on gold, few attempts have been made to investigate theoretically the physisorption state and its transition to chemisorption.<sup>17</sup>

Available X-ray photoelectron spectroscopy (XPS) data indicate that where liquid deposition of thiol SAMs on GaAs (001) is used, surface conditions are close to stoichiometric.<sup>10</sup> However, the use of etching agents in preparation steps preceding thiol deposition suggests that the surface may be highly disordered. The atomic level morphology of such a surface is not known, and thus, the results of modeling of such conditions are impossible to compare with experiment unambiguously. To avoid this problem, we chose to investigate the ideally reconstructed surfaces of GaAs, which are directly

achievable in a vacuum. We used H<sub>2</sub>S adsorption on GaAs as a test case since it is very similar to thiol chemically and since a significant body of experimental data is available for this material system.<sup>18,19</sup> To verify the accuracy of our calculations and to compare thiol deposition on GaAs with the more extensively studied gold case, we also performed calculations of thiol physisorption on gold.

## 2. Computational Details

Calculations were performed in a periodic supercell approach using the SIESTA code.<sup>20</sup> Details on the modeling parameters can be found in our previous study.<sup>21</sup> In short, we used a 300 Ry cutoff for density, double- $\xi$  plus polarization basis (DZP), and relativistic pseudo-potentials with non-linear core-corrections (NLCC). Basis set superposition error (BSSE) corrections were applied in all binding energy calculations. As compared to our previous study, several important improvements were made. First, the back side of the GaAs slab was saturated with pseudo-hydrogen atoms with a partial ion charge, in contrast to real hydrogen. Second, the vacuum region was increased to 30 Å since it is fairly computationally inexpensive to model with the localized basis sets. The surface of GaAs was modeled using 8–9 layer slabs with a  $\xi(4 \times 2)$  reconstruction for Ga-rich conditions<sup>22–24</sup> and a  $\beta 2(2 \times 4)$  reconstruction for As-rich conditions.<sup>24</sup> Calculations with a  $\beta 2$  structure for Ga-rich conditions were also performed, but they were unable to explain the observed experimental data, similar to the modeling results of Cl<sub>2</sub> adsorption on the Ga-rich GaAs (001) surface.<sup>25</sup> A  $(5 \times 3)$   $k$ -grid was used for the  $(2 \times 4)$  surface unit cell. The gold (111) surface was modeled using a 6 layer slab with 12 atoms in a layer and a  $(6 \times 7)$   $k$ -grid. No 3d states were included in the valence states for Ga and As, while 5d states were included for gold.

Density functional theory (DFT) is known to incorrectly describe van der Waals (vdW) interactions. A comparative study of different exchange-correlation functionals has shown that the generalized gradient approximation (GGA) cannot reproduce vdW attractions between carbon-containing molecules at all, while the local density approximation (LDA) provides interac-

\* Corresponding author. E-mail: jan.j.dubowski@usherbrooke.ca.

tion energies close to experimental ones.<sup>25</sup> Although this happens due to a cancellation of errors rather than due to a more correct description, LDA is often used to study weak interactions (e.g., those between organic molecules and carbon nanotubes<sup>26</sup>).

Both LDA and GGA in the Perdew–Burke–Ernzerhof formulation (PBE96)<sup>27</sup> were used in this study. Our calculations using the PBE functional did not show any attraction between thiol chains but described correctly the bond strengths in these molecules.<sup>21</sup> In contrast, LDA provides thiol–thiol interaction energies and distances similar to those reported using empirical molecular mechanics calculations.<sup>28</sup> However, LDA strongly overestimates the chemical binding energies. For example, the LDA calculated value for the S–H bond in thiol is 4.30 eV, which compares to 3.78 eV calculated with the PBE functional. Henceforth, all reported calculation results were performed using the PBE functional, unless indicated otherwise.

### 3. Results

**3.1. Need for Physisorbed Precursor.** Available experimental temperature programmed desorption (TPD) data show that short-chain thiols desorb intactly from GaAs (110)<sup>7</sup> and Ga-rich (001)<sup>8,9</sup> surfaces at around room temperature. However, the second-order desorption kinetics and desorption activation energy of 0.8–1 eV, which is too high for vdW interactions, suggest that the S–H bond is cleaved upon adsorption and is re-established upon desorption.

Previously, we reported an S–As bond energy of 2.1 eV (for the case of thiolate on As-rich (2 × 1) reconstructed (001) GaAs),<sup>21</sup> which is much weaker than the S–H bond of 3.78 eV. The relative strengths of these bonds could be predicted even without performing *ab initio* calculations, based on the smaller covalent radius of H and, consequently, its shorter bond with S. A well-known empirical rule predicts that, with the exception of some special cases, shorter bonds are stronger.<sup>29</sup>

It is energetically unfavorable to break the S–H bond and replace it with a sulfur–surface bond and a free hydrogen atom. Adsorption of hydrogen on the surface brings the lacking energy and makes chemisorption of thiols possible. To cleave the S–H bond, both S and H should appear simultaneously close to the surface atoms. However, our molecular dynamics simulations have shown that for thiols approaching the surface, this is a very rare event. Being significantly lighter than sulfur and experiencing steric repulsion from the surface, H bounces away before S approaches close enough to the surface. Nevertheless, if the molecule is physisorbed, both hydrogen and sulfur stay close to the surface for a sufficient period of time, enabling S–H bond cleavage. A higher probability of adsorption at lower temperatures reported for thiols on gold<sup>15,16</sup> and hydrogen sulfide on GaAs<sup>19</sup> is indicative of the physisorbed precursor needed for transition to chemisorption. At lower temperatures, more molecules are able to stick to the surface and remain physisorbed for a longer time. The rates of molecular desorption and of transition to chemisorption are defined by the physisorption energy and the height of the transition barrier, respectively. The physisorption energy depends on thiol length and reaches 1.08 eV for decanethiol on gold.<sup>15</sup>

**3.2. Adsorption Site.** Experimental high-resolution electron energy loss spectra (HREELS) of H<sub>2</sub>S adsorbed on the GaAs (001) surface at 100 K show only the presence of As–H bonds and no Ga–H bonds,<sup>19</sup> suggesting that S binds preferentially to Ga even on an As-rich surface. A similar conclusion was made based on XPS data,<sup>18</sup> which show the presence of sulfur on the surface but no sulfur-associated shifts in the As 3d spectrum upon annealing to 600 K, despite the presence of shifts

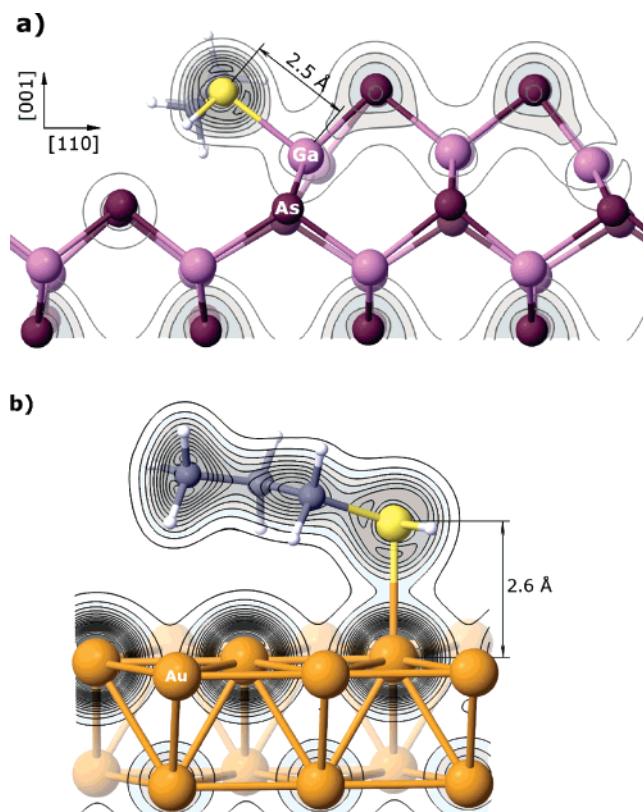


**Figure 1.** Electron density in the plane of the S-surface non-dissociative chemical bond for propanethiol adsorbed on (a) As-rich  $\beta(2 \times 4)$  GaAs (001) surface and (b) Au (111) surface. Isocontour step is 0.025 atomic units (au).

at lower temperatures. The preferential adsorption of Br on the Ga sites was also reported in an STM study of the As-rich GaAs (001) surface exposed to Br<sub>2</sub>.<sup>30</sup> Other halogens are also known to etch the GaAs surface via removal of gallium halides.<sup>23,31</sup>

Our GGA calculations of H<sub>2</sub>S as well as thiol adsorption on GaAs revealed a stronger attraction of sulfur to Ga sites, with a binding energy of 0.19 eV in contrast to zero energy for binding to As sites. This suggests that the attraction is not due to a pure vdW interaction but due to the formation of a chemical bond. The LDA calculations give thiol binding energies of 0.47 and 0.15 eV to the Ga and As sites, respectively. Assuming that the vdW interaction is of the same strength on Ga and As sites and is better reproduced in LDA, while chemical binding is better reproduced in GGA, we can estimate a total binding energy of 0.15 + 0.19 = 0.34 eV for Ga sites and 0.15 eV for As sites. The former value varies depending on the surface reconstruction and the specific adsorption site (there are three non-equivalent Ga sites on the Ga-rich  $\xi(4 \times 2)$  surface).

A similar conclusion can be made based on experimental physisorption energies of thiols on gold. The contribution of SH–surface interactions to the total physisorption energy is 0.34 eV, which is much stronger than 0.06 eV per CH<sub>2</sub> unit.<sup>15</sup> This suggests that the SH–surface interaction is not a pure vdW attraction.

Figure 1 shows the isocontours of valence electron density between sulfur and surfaces of (001) GaAs and (111) Au. There is no minimum in the electron density between S and Ga, which is indicative of the chemical bond formation.<sup>32</sup> Although there is a minimum between sulfur and gold, the formation of a bond is clearly visible since the S–Au distance of 2.6 Å (LDA) is much smaller than the sum of vdW radii of 3.46 Å. The presence

of this minimum can be explained by the fact that Au 5d semi-core states were actually included as valence states in our calculations.

A short sulfur–surface bond forces thiols to bend on both GaAs and Au since the rest of the chain is not allowed to approach closer to the surface due to steric repulsion. Our geometry of thiol on gold slightly differs from that reported previously,<sup>33</sup> where the thiol chain stayed straight with the end group lifted farther from the surface. Such a configuration was obtained due to the different geometry constraints used for relaxation of the structure. If a Z-matrix is used to define the thiol atomic coordinates, the angles between bonds are fixed, and thus, the chain is kept straight. This will force the thiol to go up due to the short S–Au bond and steric repulsion of the first CH<sub>2</sub> unit from the surface. As a consequence, the physisorption energy would be underestimated, especially for longer chain thiols, since most of the CH<sub>2</sub> units and the CH<sub>3</sub> end group would be located too far from the surface to feel the vdW attraction. In our calculations, we did not impose any constraints during geometry relaxation. This resulted in a thiol extending flat on the surface with a chain slightly bended near sulfur. Such an approach complicates finding the global energy minimum and consequently the right adsorption site and geometry, as was reported for the chemisorption state of thiols on gold.<sup>34</sup> To avoid this problem and to find the relaxed geometries for both physisorption and chemisorption states, we used molecular dynamics simulations.

In the case of chemisorption, where the sulfur–surface bond becomes even shorter and has a preference to lie in the S–C–C chain plane, thiol bending would be even stronger. This can result in a detachment of the rest of the chain from the surface, especially if its attraction to the surface is not strong enough. In contrast to gold, thiol chain bending on GaAs is smaller, while surface relaxation is much more pronounced. In this case, the surface Ga atom lifts in the direction of changing hybridization from sp<sup>2</sup> to sp<sup>3</sup> (see Figure 1a), which indicates an accumulation of charge on Ga. However, this relaxation is not as pronounced as in the case of chemical bond formation upon S–H cleavage.

To understand the nature of the non-dissociative sulfur–surface bond, we investigated the projected density of states and charge redistribution upon thiol adsorption. First, it is instructive to highlight the electronic configuration of sulfur and its orbital configuration in thiols. The electronic configuration of sulfur is 3s<sup>2</sup>3p.<sup>4</sup> Two unpaired p-electrons participate in the formation of the bonds with H and C in thiol, while another two p-electrons form a lone pair, which becomes the highest occupied molecular orbital (HOMO) of the molecule. The s-orbitals do not hybridize with p-orbitals; thus, H–S and S–C bonds form a nearly right angle, and the lone pair is perpendicular to the H–S–C plane. Hydrogen sulfide has an identical configuration, with the only difference being that the S–C bond is replaced with another S–H bond.

From the projected density of states, it can be seen that the thiol HOMO shifts upon adsorption to lower energies and broadens significantly, indicating its participation in chemical bonding. The electron density redistribution presented in Figure 2 shows the transfer of charge from a sulfur lone pair orbital to an empty Ga dangling bond, confirming the formation of the bond between Ga and S. The presence of such a hydrogen-like bond was predicted from experimental data of thiol adsorption on GaAs (110),<sup>7</sup> and similar conclusions were made from calculations of thiol on gold.<sup>33</sup> Thus, it is more correct to refer to this as a chemisorption state since physisorption by definition

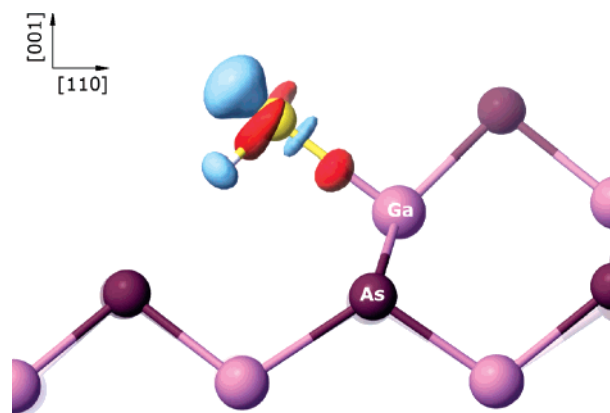


**Figure 2.** Regions of loss (light blue) and gain (red) of electron density induced by adsorption of thiol on As-rich  $\beta 2(2 \times 4)$  GaAs (001) surface. Isodensity surfaces correspond to  $\pm 0.005$  au.

is purely due to vdW interactions. However, we will continue to use the term physisorption further in the text to avoid confusion between the two chemisorption states (dissociative and non-dissociative).

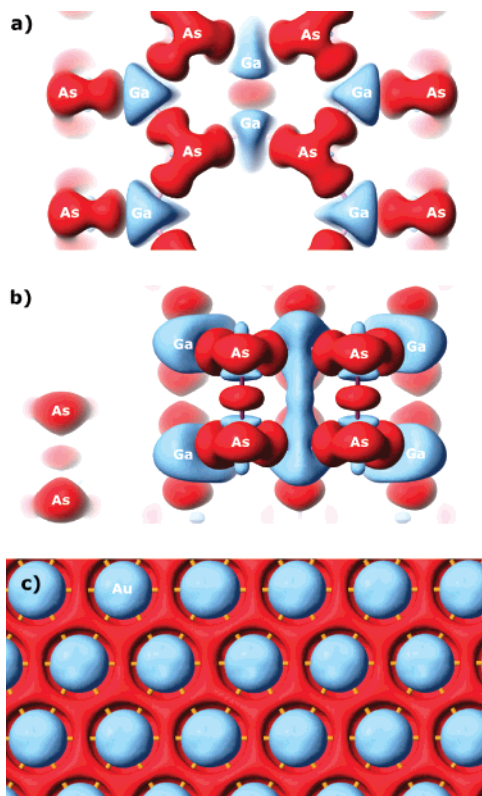
We attempted to find a correlation between the possible adsorption sites and the electronic properties of the surface to predict the adsorption site without performing structure relaxations with a molecule over each available site. Our initial guess was to monitor the regions where the electrostatic potential of the surface is of the opposite sign to that of the sulfur lone pair. This worked for most cases but predicted incorrect behavior of thiols on gold and on As-rich GaAs surfaces without Ga sites, such as the  $c(4 \times 4)$  reconstruction or a disordered As overlayer. A better correlation was found when using differential electron density, defined as  $\Delta\rho = \rho_{\text{system}} - \sum\rho_{\text{freeatoms}}$ , which describes the charge redistribution upon formation of the system (molecule, surface, etc.).

Figure 3 shows the differential density for different GaAs surface reconstructions and for the Au (111) surface. We found that thiol readily binds to sites with a negative differential density (light blue regions in Figure 3) (i.e., to those depleted of charge). This suggests that atoms with a lack of electrons are ready to accept extra charge donated by sulfur, allowing them to return to a more bulk-like state. Positive differential density (red regions in Figure 3) is indicative of bond formation or a filled dangling bond, while charge depletion (light blue regions in Figure 3) indicates empty dangling bonds. Strictly speaking, for metallic gold, it is more correct to use the phrase charge depletion on surface atoms, in contrast to dangling bonds common for semiconductors.

The directionality of the orbitals forming this weak chemisorptive bond forces the thiol chain to extend parallel to the surface on both Au and GaAs substrates. Consequently, the formation of a SAM would require cleavage of the S–H bond.

**3.3. Transition Barrier from Physisorption to Chemisorption.** Calculations reported in this section were performed using LDA. While the calculated binding energies are greater than those given by GGA, the energetic barriers do not differ much between the two approximations.

Looking at the thiol adsorption geometries in Figures 1a and 2, we can see that while S is already situated close to Ga (bond length is 2.5 Å as compared to 2.3 Å in the chemisorbed state with a cleaved S–H bond<sup>21</sup>), H appears to be close to a nearby As. On As-rich  $\beta 2(2 \times 4)$  surfaces, the distance from H to As is 2.65 Å. However, we wanted to find the distance the hydrogen atom needs to overcome to become adsorbed on the surface. Consequently, we measured from the position of H bound to S



**Figure 3.** Regions of loss (light blue) and gain (red) of electron density induced by the formation of the surface: (a) Ga-rich  $\xi(4 \times 2)$ , (b) As-rich  $\beta(2 \times 4)$ , and (c) Au (111). Isodensity surfaces correspond to  $\pm 0.003$  au.

to the position of H chemisorbed on As. This distance was  $\sim 2$  Å and was expected to be easily overcome even below room temperature. Our molecular dynamics simulations demonstrated that due to thermal vibrations, the hydrogen atom can approach As close enough to become more strongly attracted to it than to S, which resulted in the breaking of the S–H bond. The barrier for this transition was found to be  $0.5 \pm 0.3$  eV. Strong energy oscillations due to the vibration of all other atoms precluded its exact determination. Consequently, we recalculated this situation, allowing only the hydrogen atom to move. The position of H was sequentially fixed in different points along the straight path that connects the relaxed initial (physisorption) and final (chemisorption) states. All other atoms were allowed to relax. For each fixed H position, the starting geometry for relaxation was taken as that of thiol physisorbed on the surface, which guarantees that we do not artificially lower the barrier and that the relaxed geometry is directly reachable from the initial one.

An important question that arises is whether thiol dissociates into a proton and thiolate ion ( $\text{RS}^-$ ) or into neutral hydrogen and a thiyl radical ( $\text{RS}^\bullet$ ). For the intermediate position corresponding to the highest point of the barrier, we found that the electron density around hydrogen does not change significantly (i.e., H stays neutral). This is consistent with the much lower energy of 3.78 eV needed for dissociation into a neutral hydrogen and a thiyl radical than the 15.3 eV required for dissociation into  $\text{RS}^-$  and  $\text{H}^+$ , although, in liquid solutions, the latter reaction may become more favorable due to the additional energy gain associated with solvation. Nevertheless, to reference the thiol part adsorbed on the surface, the term thiolate is widely used in the literature,<sup>9,16,33</sup> as well as in this paper, even though the molecular part is neither an ion nor a radical.

The calculated transition barrier heights for  $\text{H}_2\text{S}$  on Ga-rich  $\xi(4 \times 2)$  and As-rich  $\beta(2 \times 4)$  reconstructed surfaces were 0.3 and 0.2 eV, respectively, both of which resulted in dissociative adsorption at around 120 K. The barrier on the Ga-rich surface was higher since the surface is rather flat and the distance that hydrogen is required to overcome to become chemisorbed is greater than that on the As-rich surface. For thiols, the barrier height of  $\sim 0.5$  eV is slightly greater, despite the weaker S–H bond as compared to that in  $\text{H}_2\text{S}$ . This is due to energy losses related to thiol bending and a less favorable chemisorption geometry, in which the S–Ga bond does not lie in the plane of the S–C–C chain. Calculated barrier heights are close to the experimentally determined value of 0.3 eV for thiols on gold.<sup>15</sup>

In a weakly chemisorbed state with S over Ga, cleaved hydrogen can in principle adsorb not only on As but also on nearby Ga. However, the 4 Å distance to Ga is twice that to As, suggesting a higher barrier for chemisorption. What is even more important, the resulting chemisorption geometry with S and H on two Ga atoms is 0.2 eV higher in energy than that of free thiol molecule. It is interesting to note that for geometries where S is situated elsewhere than above Ga, with the molecule physisorbed via pure vdW interactions, the transition barrier to chemisorption is not higher. However, similar to the adsorption on two Ga sites, the resulting chemisorption states are found to be unstable and will easily recombine. This suggests that on vacuum-prepared GaAs (001) surfaces, hydrogen would always adsorb to As, in agreement with experimental observations.<sup>19</sup> It also clarifies the interpretation of XPS data:<sup>18</sup> sulfur indeed binds only to Ga, while the shifts observed in As 3d spectra are related to As–H bonds.

**3.4. Comparison to Experimental Data.** To estimate the accuracy of our calculations, we compared our results with available experimental data for hydrogen sulfide and short-chain thiols. We concentrated on XPS<sup>18</sup> and HREELS data<sup>19</sup> and will discuss the main features of TPD spectra for  $\text{H}_2\text{S}$ <sup>18,19</sup> and thiols.<sup>8,9</sup>

Table 1 summarizes the experimental TPD data<sup>18,19</sup> and the results of our calculations for  $\text{H}_2\text{S}$  desorption from the Ga-rich GaAs (001) surface. Hydrogen sulfide also was observed to desorb molecularly from the GaAs (001) surface at around room temperature, although its dissociation is clearly visible from available HREELS<sup>19</sup> and XPS<sup>18</sup> data. Lower coverages obtained with the 300 K deposition in vacuum, as compared to the 100 K deposition, suggest the presence of a physisorbed precursor, which undergoes transition to chemisorption upon annealing.

It was found experimentally that the  $\text{H}_2\text{S}$  decomposition temperature was greater than the 117 K temperature of the physisorption peak observed in TPD spectra.<sup>19</sup> However, TPD spectra recorded for deposition at 100 K using different  $\text{H}_2\text{S}$  doses show that the physisorption peak at 117 K populates only after saturation of the recombinative desorption peak at 400 K. This implies the presence of two physisorption states: one of which is strong enough to survive the  $\text{H}_2\text{S}$  decomposition temperature and completely transforms to chemisorption upon annealing and the second one desorbing at 117 K. Saturation coverage for the latter state was found to be less than one monolayer and clearly ruled out multilayer adsorption.<sup>19</sup> Our results indicate that these two different states could in fact correspond to non-dissociative chemisorption on Ga sites and physisorption elsewhere. Observed shifts in sulfur XPS data at 90 K confirmed the presence of two different physisorption states of  $\text{H}_2\text{S}$ . These states were assigned to physisorption on Ga and As atoms, based on their different electronegativities.<sup>18</sup>

**TABLE 1: Experimental Temperatures of Desorption Peaks<sup>18,19</sup> and Calculated Recombination Energies of H<sub>2</sub>S from the Ga-Rich Surface**

temp (K)	feature	energy (eV) <sup>a</sup>	suggested mechanism	calcd energy (eV)
117	narrow peak at high exposures	0.3	physisorbed H <sub>2</sub> S	0.15 (LDA)
170	peak at low exposures, shoulder at high exposures	0.44	weakly chemisorbed H <sub>2</sub> S	0.47 (LDA) 0.34 (LDA + GGA)
250–400	broad peak	0.67–1.09	SH + H	0.85 (GGA)

<sup>a</sup> Experimental energies were recalculated from original temperatures and heating rates, using a simplified Redhead formula,<sup>37</sup> assuming first-order kinetics and a pre-exponential factor of 10<sup>13</sup> Hz.

We anticipate that physisorption on different surface atoms would not result in significantly different XPS shifts for sulfur since vdW interactions do not involve charge transfer; hence, we claim that our interpretation is more correct. Our estimated binding energy of 0.34 eV for H<sub>2</sub>S over the Ga site is close to the 170 K feature in the TPD spectra (see Table 1) and supports our conclusions.

The saturation coverage of H<sub>2</sub>S was found to be the same on As- and Ga-rich surfaces for the case of 100 K deposition.<sup>19</sup> Coverage was found to decay with increasing deposition temperature, as expected for adsorption involving a physisorbed precursor. For deposition at room temperature, a lower coverage was observed on As-rich as compared to Ga-rich surfaces,<sup>19</sup> despite the slightly smaller transition barrier on the former, as indicated by our calculations. The resulting chemisorption state on As-rich surfaces was calculated to be only 0.2 eV lower than the physisorption state, in contrast to a 0.5 eV difference on Ga-rich surfaces, suggesting an easier desorption from the As-rich surfaces in agreement with experimental data.

A relatively low coverage of 0.57 monolayers of H<sub>2</sub>S on the GaAs surface was estimated from XPS data.<sup>18</sup> This low coverage also was expected for thiol adsorption. For instance, a  $p(2 \times 2)$  LEED structure, achieved upon repeated exposure to thiol and annealing to 750 K,<sup>9</sup> implies that the surface concentration of chemisorbed sulfur could reach 0.25 monolayers. Such a low coverage is in agreement with our findings that H<sub>2</sub>S and thiol adsorption requires two surface sites for binding S and H; moreover, only specific combinations of sites are allowed.

Figure 4 shows the relaxed geometries of the free Ga-rich  $\xi(4 \times 2)$  surface and chemisorbed H<sub>2</sub>S molecules on it. We find that dissociation is energetically favorable only when the resulting S and H occupy the Ga and As sites, respectively, but not on any pair of them. For example, dissociation on Ga2 and As3 (see Figure 4) is not favorable. There are 4 Ga sites in the  $\beta 2(2 \times 4)$  surface unit cell of the As-rich surface (Figure 1a) and 6 Ga sites in the  $\zeta(4 \times 2)$  reconstruction (Figure 4). However, adsorption of H<sub>2</sub>S or thiols on the central Ga dimer of the Ga-rich surface, which is slightly below the surface level (atom 4 in Figure 4), is prohibited at low coverage due to steric repulsion from the nearby As3 atoms. At higher coverage, when the 4 available Ga2 sites are populated, the surface geometry changes to accommodate the newly formed sp<sup>3</sup> hybridization of the As1 atoms and Ga2 atoms, resulting from the adsorption of H and SH (see Figure 4b). This configuration also allows the As3 atom to change the hybridization to sp<sup>3</sup> without breaking any bonds, which raises the central Ga4 dimer above the surface and opens it for further adsorption of H<sub>2</sub>S. However, a new hydrogen sulfide molecule does not dissociate to cover both atoms of the dimer. Instead, it transfers its H atom without any energy barrier to the SH species chemisorbed nearby (arrows in Figure 4b,c), transforming it into physisorbed H<sub>2</sub>S. This molecule cannot dissociate since all favorable nearby sites for H adsorption are already occupied. Note that the amount of physisorbed and chemisorbed species does not change, they simply exchange places. Such a process agrees with the absence of Ga–H bonds in experimental HREELS data.<sup>19</sup> It can also

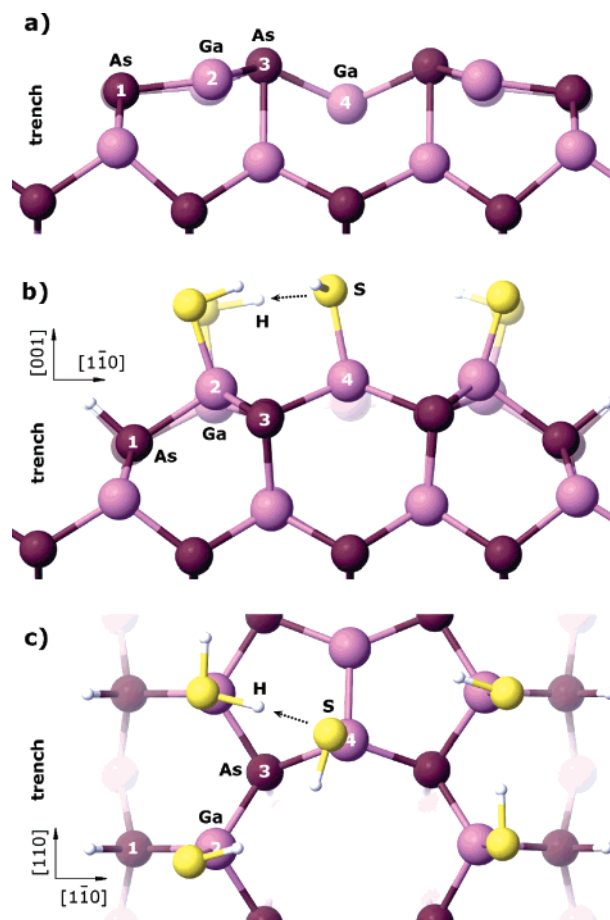


**Figure 4.** Adsorption geometries of H<sub>2</sub>S on the Ga-rich  $\xi(4 \times 2)$  surface: (a) side view of the free surface and (b and c) side and top views, depicting 1 physisorbed and 4 chemisorbed molecules.

explain the presence of the 170 K feature in the H<sub>2</sub>S desorption spectra at higher exposures<sup>18,19</sup> (see Table 1), which suggests the presence of physisorbed molecules, despite the fact that such a temperature is sufficient to transform them into chemisorbed species.

Figure 5 shows the main pathways of H<sub>2</sub>S and H<sub>2</sub> desorption from the Ga-rich surface. The calculated energy needed for SH recombination with the closest available H is 0.85 eV (Figure 5b, but where H remains on As atom 2). This corresponds perfectly to the center of a broad peak at 320 K in H<sub>2</sub>S desorption spectra.<sup>18</sup> A similar peak, which is likely of the same origin, was observed at 400 K in another TPD study.<sup>19</sup> The slightly higher temperature is probably due to a different heating rate used for those experiments. We find that more complex mechanisms of recombinative molecular desorption are also possible, explaining the broad nature of the peak. For example, recombination of SH with the H from another SH species and immediate recombination of the resulting S with a nearby H on the surface (Figure 5b, with H staying on As atom 1) requires an energy of 0.9 eV.

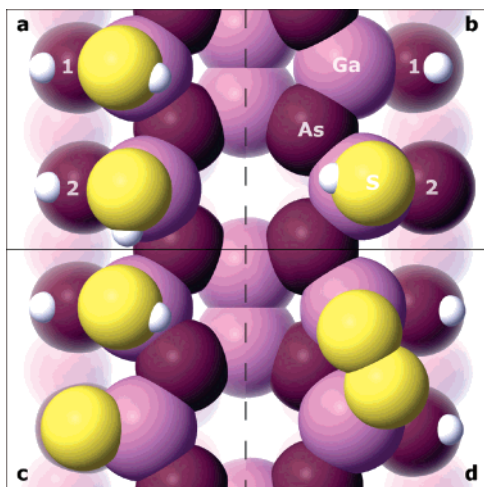


**Figure 5.** Top view of the relaxed geometries of  $\text{H}_2\text{S}$  decomposition and desorption products on the Ga-rich  $\xi(4 \times 2)$  surface: (a) starting geometry with two dissociatively chemisorbed  $\text{H}_2\text{S}$  molecules, (b) surface after recombinative desorption of one of the  $\text{H}_2\text{S}$  molecules, (c) surface after recombination of  $\text{H}_{\text{surf}}$  with  $\text{H}_{\text{SH}}$ , and (d) surface after recombination of two  $\text{H}_{\text{SH}}$  atoms. Solid lines indicate the boundaries of  $\xi(4 \times 2)$  surface unit cells. The vertical dashed line shows the reflection symmetry plane of a free surface.

In Table 2, we compare experimental desorption peak temperatures of  $\text{H}_2$  from the Ga-rich surface with our calculated energies corresponding to specific recombination mechanisms. The molecular hydrogen desorption spectrum following  $\text{H}_2\text{S}$  deposition exhibits two broad features at 350 and 480 K. The lower temperature peak was assigned to the recombinative desorption of H from the SH species with the H present on the surface (Figure 5c).<sup>18</sup> Our calculated energy of 0.88 eV for this process coincides very well with the experimental peak position. The second peak was attributed to the recombinative desorption of hydrogen atoms adsorbed on the surface<sup>18</sup> (i.e., H atoms on As1 and As2 in Figure 5a). However, our calculations show that on the Ga-rich  $\xi(4 \times 2)$  surfaces, such a reaction requires at least 1.5 eV ( $\sim 550$  K), in agreement with  $\text{H}_2$  desorption spectra after ethanethiol deposition.<sup>9</sup> We find that the recombinative desorption of  $\text{H}_2$  from the two SH species, leaving a sulfur dimer on the surface (Figure 5d), requires only 1.2 eV, which corresponds to a temperature of 445 K (see Table 2). The absence of this peak in the spectra following thiol deposition is expected since the amount of SH species on the surface in this case is much smaller than after  $\text{H}_2\text{S}$  decomposition.<sup>8,9</sup> Thus, only direct surface hydrogen recombination is possible after thiol deposition, while after  $\text{H}_2\text{S}$  adsorption, this process is less efficient and only contributes to the observed broadening of the peak at 480 K.

Experimental data suggest that recombinative desorption of  $\text{H}_2\text{S}$  corresponds to only a small fraction of deposited molecules, while the rest of the molecules dissociate irreversibly, resulting in sulfur deposition on the surface.<sup>19</sup> We find that direct dissociation of SH species on the surface requires  $\sim 2$  eV (i.e.,  $\sim 720$  K) for the initial geometry illustrated in Figure 5a. Thus, the observed surface sulfur at room temperatures is mainly formed via  $\text{H}_2$  recombination from two SH species, as discussed previously. The resulting sulfur tends to form dimers or to bind to two surface atoms to avoid the formation of double bonds with the surface (Figure 5c,d). These and other similar processes may lead to the creation of empty dangling bonds on unoccupied surface atoms, making possible the adsorption of  $\text{H}_2\text{S}$  on As sites. As a result, H can be adsorbed on Ga, as observed

experimentally for room-temperature deposition, but not at low temperatures.<sup>19</sup>

The recombinative desorption energy for thiols was calculated to be 0.85 eV, which is slightly lower than the experimental value of 0.95 eV.<sup>9</sup> It should be noted that our calculated recombinative desorption energies on As-rich  $\beta 2(2 \times 4)$  surfaces (0.55 eV for  $\text{H}_2\text{S}$  and 0.35 eV for thiol) are much smaller than those on Ga-rich surfaces. Unfortunately, no experimental data are available to verify these results with the exception of sulfur coverage differences observed between As- and Ga-rich surfaces following  $\text{H}_2\text{S}$  deposition at room temperature, as discussed previously.

The process of desorption is quite complex for  $\text{H}_2\text{S}$ . The energetics of recombination varies strongly depending on the occupation of the sites within the unit cell. This highlights the importance of the adsorption kinetics, which determines the adsorption site for each species. For thiols, even a significantly greater number of possibilities exists for both decomposition and recombination reactions.<sup>8,9</sup> Their energetics and the factors affecting specific binding energies require further investigation.

**3.5. Physisorption Energy versus Chain Length.** The LDA calculated physisorption energies of thiols on GaAs are shown in Figure 6. To estimate the accuracy of our values, we also performed similar calculations for thiols on gold and compared them with available experimental values.<sup>15</sup> Our LDA results slightly overestimate the vdW interactions between thiols and surface. However, they are much closer to experimental data than previously reported calculations,<sup>17,33,35</sup> performed only for short-chain thiols in GGA. Presented results for GaAs are much more scattered than for gold since many more adsorption geometries are possible and different surface reconstructions exist. Open circles and a thin solid line in Figure 6 correspond to adsorption on a relatively flat Ga-rich surface, when sulfur forms a weak chemical bond to Ga. This situation corresponds most closely to the nature of thiol adsorption on gold, and it should be considered as such when comparing the interaction strengths on gold and GaAs surfaces. Calculated results show a slightly stronger vdW attraction of thiols to GaAs than to gold, consistent with the larger vdW radii of Ga and As.

Open diamonds in Figure 6 show the upper limit of physisorption energies obtained when thiol is adsorbed along the trench between As dimers (see Figures 1a and 2), effectively increasing the number of atoms that participate in vdW interactions. Open triangles in Figure 6 show the lower limit of energies, achieved for thiol lying over As dimers on As-rich  $\beta 2(2 \times 4)$  reconstruction, with sulfur situated over the As site (i.e., not forming a bond to the surface with its lone pair orbital). Surface roughness reduces the number of thiol  $\text{CH}_2$  units that appear close enough to the surface to feel the vdW attraction by a factor of 2. Similar values are expected for disordered surfaces achieved after liquid etching. For the case of Ga-rich surfaces, approximate values of the contribution of different thiol parts into the total physisorption energy are as follows: 0.34 eV for the SH head group, 0.2 eV for the  $\text{CH}_3$  end group, and 0.14 eV per  $\text{CH}_2$  unit. In general, physisorption energies on GaAs are comparable to that on gold.<sup>15</sup>

#### 4. Discussion

Apart from the proof for the need of a physisorbed precursor, our results also highlight several new important findings. For example, we have shown that thiols and hydrogen sulfide have a preference for binding to Ga empty bonds on an ideally reconstructed surface. This is in contrast to a widely used suggestion that thiols preferentially bind to As sites.<sup>10,36</sup> This

**TABLE 2: Experimental Temperatures of Desorption Peaks and Calculated Recombination Energies of H<sub>2</sub> from the Ga-Rich Surface Following H<sub>2</sub>S<sup>18,19</sup> and Thiol Deposition<sup>8,9</sup>**

temp (K)		feature	energy (eV) <sup>a</sup>	suggested explanation	calcd energy (eV)
H <sub>2</sub> S	thiols				
250–400		shoulder	0.67–1.09	H <sub>SH</sub> + H <sub>surf</sub>	0.88
400–600		broad peak	1.09–1.66	H <sub>SH</sub> + H <sub>SH</sub>	1.2
	550–600	broad peak	1.47–1.59	H <sub>surf</sub> + H <sub>surf</sub>	1.5

<sup>a</sup> Experimental energies were recalculated from original temperatures and heating rates, using a simplified Redhead formula,<sup>37</sup> assuming first-order kinetics and a pre-exponential factor of 10<sup>13</sup> Hz.

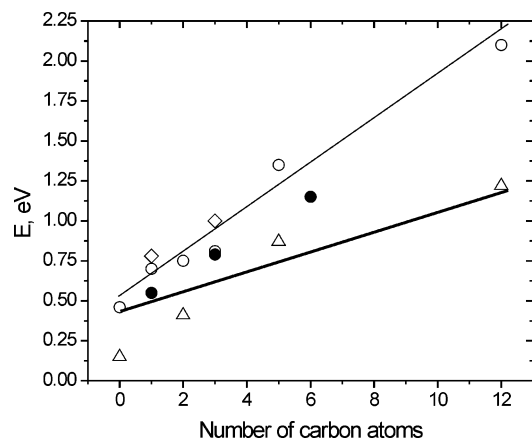


**Figure 6.** Dependence of the physisorption energy on thiol chain length. Bold line: experimental results (line approximated) for Au (111)<sub>15</sub> and solid circles: our calculations for Au (111). Open symbols: our calculations for different GaAs (001) surface reconstructions. Open circles: adsorption on Ga-rich  $\xi(4 \times 2)$  (a thin line is a guide for the eye); open diamonds: adsorption along a trench between As dimers on As-rich  $\beta 2(2 \times 4)$  surface; and open triangles: adsorption over dimers on As-rich  $\beta 2(2 \times 4)$  surface.

suggestion is based on XPS data for As-enriched surfaces passivated with different sulfides<sup>1</sup> or on the fact that arsenic ions can form mercaptide with thiol derivatives.<sup>36</sup> Our calculations show that the strength of S–Ga bonds for thiolate chemisorbed on the surface is comparable to that of S–As. However, slightly more favorable energetics and the presence of an intermediate weak chemisorption state, which is due to an overlap of the sulfur lone pair with an empty Ga dangling bond, result in the preferential adsorption of thiols on Ga. We expect this to be true also for (110) surfaces, obtained by cleavage of the samples in vacuum<sup>7</sup> or in solution,<sup>36</sup> where equal amounts of Ga empty and As filled dangling bonds exist. For nearly stoichiometric but disordered surfaces obtained using liquid etching,<sup>10</sup> the presence of Ga atoms on the surface would inevitably result in binding of sulfur to them, although this does not preclude the formation of S–As bonds as well. The XPS reports do not provide enough information for unambiguous determination of the origin of binding energy shifts, as we have shown using the example of H<sub>2</sub>S adsorption. Available XPS data for liquid deposition of thiol SAMs on GaAs are controversial, with reports of As–S bonding<sup>10,13</sup> or, by contrast, unresolved Ga–S or As–S bonding.<sup>8,12</sup> It should be noted that observed shifts in As binding energies could be partially caused by the presence of As–H bonds, as we have shown that hydrogen desorption is a very unfavorable process, at least on surfaces prepared in a vacuum.

The preference for S–Ga bonding and the impossibility of chemisorption on some sites due to geometrical constraints (i.e., on the central Ga dimer of the clean  $\xi(4 \times 2)$  reconstructed surface) prohibit part of the adsorption configurations from being realized, even the energetically favorable ones. This defines a strict sequence of chemisorption events and highlights the

importance of adsorption kinetics. The energetics and geometrical requirements that H should stay on the surface and adsorb on a surface species different from that of S, coupled with the fact that not all of the Ga–As pairs are favorable for chemisorption, add additional constraints to the process of adsorption. For the investigated ideally reconstructed surfaces, this means that a high coverage with thiols is not possible, precluding high-quality SAM formation.

Obtained values of the transition barrier heights (0.2–0.3 eV for H<sub>2</sub>S and ~0.5 eV for thiols) are comparable to the physisorption energies of H<sub>2</sub>S and short-chain thiols. These values define the thiol chemisorption and desorption rates, increasing the probability of adsorption for longer thiols and for lower deposition temperatures. Taking into account that the resulting chemisorption state is calculated to be only 0.2–0.5 eV lower than the physisorption state (depending on surface reconstruction), the inverse transformation from the chemisorption to the physisorption state is possible, if after S–H cleavage the rest of the chain stays physisorbed on the surface. Such a process would require less energy than the recombinative desorption of thiol. This reduces the chemisorption rate for longer thiols, in contrast to shorter chain thiols that stay attached to the surface only via a sulfur–surface bond.

We find that the main difference of thiol adsorption on GaAs from that on gold is that hydrogen stays on the GaAs surface, while on gold, it desorbs as molecular hydrogen. For GaAs (001) surfaces, room temperature is not sufficient for H<sub>2</sub> desorption; however, it can induce thiol recombination with surface hydrogen. This suggests that to improve the stability of deposited thiols, successful preparation procedures should not allow hydrogen adsorption on the surface. This might be possible, for example, by using laser dissociated disulfides as a source of thiols. More possibilities could be suggested for deposition from the liquid phase, for example, dissociation of thiols in solution and anodization of the substrate or a selective chemical reaction to remove hydrogen from the surface.

## 5. Conclusion

We carried out ab initio calculations of the physisorption state and the kinetics of transition to chemisorption for hydrogen sulfide and alkanethiols on GaAs (001) surfaces and compared them to the adsorption of alkanethiols on gold. Using energetics arguments and molecular dynamics simulations, we have shown that a physisorbed precursor is essential for the adsorption of H<sub>2</sub>S and thiols on GaAs surfaces.

For deposition on ideally reconstructed GaAs surfaces, which can be achieved in a vacuum chamber, we found a preference for S–Ga bond formation due to the presence of an intermediate weak chemisorption state, resulting from the overlap of a sulfur lone pair orbital with an empty Ga dangling bond. This, coupled with the energetic constraints prohibiting the adsorption of hydrogen on Ga and on some of the As sites, allowed for a better understanding of the adsorption mechanisms involved and provided an explanation for the observed features in experimental data for H<sub>2</sub>S and thiol deposition.

The calculated transition barrier height from a physisorption to a chemisorption state for thiols on GaAs was found to be  $\sim 0.5$  eV, only slightly depending on the particular adsorption site and surface reconstruction. Physisorption energies were investigated as a function of thiol chain length and for various surface conditions. For the case of the Ga-rich  $\xi(4 \times 2)$  surface, the obtained values for the contribution from different thiol components to the total physisorption energy were as follows: 0.34 eV for the SH head group, 0.2 eV for the CH<sub>3</sub> end group, and 0.14 eV for each CH<sub>2</sub> unit. The values of transition barrier height and physisorption energies are comparable to those of thiols on gold.

**Acknowledgment.** Funding for this research was provided by the Canadian Institutes for Health Research and the Canada Research Chair Program. The calculations presented in this work were carried out using the infrastructure provided by the Réseau Québécois de Calcul de Haute Performance.

**Supporting Information Available:** 3-D structures of optimized geometries. This material is available free of charge via the Internet at <http://pubs.acs.org>.

## References and Notes

- (1) Lunt, S. R.; Ryba, G. N.; Santangelo, P. G.; Lewis, N. S. *J. Appl. Phys.* **1991**, *70*, 7449.
- (2) Moumanis, K.; Ding, X.; Dubowski, J. J.; Frost, E. H. *J. Appl. Phys.* **2006**, *100*, 34702.
- (3) Ding, X.; Moumanis, K.; Dubowski, J. J.; Frost, E. H.; Escher, E. *Appl. Phys. A* **2006**, *83*, 357.
- (4) Sackmann, E.; Tanaka, M. *Trends Biotechnol.* **2000**, *18*, 58.
- (5) Seker, F.; Meeker, K.; Kuech, T. F.; Ellis, A. B. *Chem. Rev.* **2000**, *100*, 2505.
- (6) Lodha, S.; Janes, D. B. *J. Appl. Phys.* **2006**, *100*, 024503.
- (7) Camillone, N.; Khan, K. A.; Osgood, R. M. *Surf. Sci.* **2000**, *453*, 83.
- (8) Donev, S.; Brack, N.; Paris, N. J.; Pigram, P. J.; Singh, N. K.; Usher, B. F. *Langmuir* **2005**, *21*, 1866.
- (9) Singh, N. K.; Doran, D. C. *Surf. Sci.* **1999**, *422*, 50.
- (10) Adlkofer, K.; Tanaka, M. *Langmuir* **2001**, *17*, 4267.
- (11) Jun, Y.; Zhu, X. Y.; Hsu, J. W. P. *Langmuir* **2006**, *22*, 3627.
- (12) McGuinness, C. L.; Shaporenko, A.; Mars, C. K.; Uppili, S.; Zharnikov, M.; Allara, D. L. *J. Am. Chem. Soc.* **2006**, *128*, 5231.
- (13) Neshet, G.; Vilan, A.; Cohen, H.; Cahen, D.; Amy, F.; Chan, C.; Hwang, J. H.; Kahn, A. *J. Phys. Chem. B* **2006**, *110*, 14363.
- (14) Ding, X. M.; Moumanis, K.; Dubowski, J. J.; Tay, L.; Rowell, N. L. *J. Appl. Phys.* **2006**, *99*, 54701.
- (15) Lavrich, D. J.; Wetterer, S. M.; Bernasek, S. L.; Scoles, G. *J. Phys. Chem. B* **1998**, *102*, 3456.
- (16) Schreiber, F. *Progr. Surf. Sci.* **2000**, *65*, 151.
- (17) Yourdshahyan, Y.; Rappe, A. M. *J. Chem. Phys.* **2002**, *117*, 825.
- (18) Conrad, S.; Mullins, D. R.; Xin, Q. S.; Zhu, X. Y. *Surf. Sci.* **1997**, *382*, 79.
- (19) Yi, S. I.; Chung, C. H.; Weinberg, W. H. *J. Vac. Sci. Technol., A* **1997**, *15*, 1168.
- (20) Soler, J. M.; Artacho, E.; Gale, J. D.; Garcia, A.; Junquera, J.; Ordejon, P.; Sanchez-Portal, D. *J. Phys.: Condens. Matter* **2002**, *14*, 2745.
- (21) Voznyy, O.; Dubowski, J. J. *J. Phys. Chem. B* **2006**, *110*, 23619.
- (22) Lee, S. H.; Moritz, W.; Scheffler, M. *Phys. Rev. Lett.* **2000**, *85*, 3890.
- (23) Lee, S. M.; Lee, S. H.; Scheffler, M. *Phys. Rev. B: Condens. Matter Mater. Phys.* **2004**, *69*, 125317.
- (24) Schmidt, W. G.; Bechstedt, F.; Bernholc, J. *Appl. Surf. Sci.* **2002**, *190*, 264.
- (25) Wu, X.; Vargas, M. C.; Nayak, S.; Lotrich, V.; Scoles, G. *J. Chem. Phys.* **2001**, *115*, 8748.
- (26) Tourmus, F.; Charlier, J. C. *Phys. Rev. B: Condens. Matter Mater. Phys.* **2005**, *71*.
- (27) Perdew, J. P.; Burke, K.; Ernzerhof, M. *Phys. Rev. Lett.* **1996**, *77*, 3865.
- (28) Ulman, A.; Eilers, J. E.; Tillman, N. *Langmuir* **1989**, *5*, 1147.
- (29) Lide, D. R. *CRC Handbook of Chemistry and Physics*, 79th ed.; CRC Press: Boca Raton, FL, 1998.
- (30) Liu, Y.; Komrowski, A. J.; Kummel, A. C. *Phys. Rev. Lett.* **1998**, *81*, 413.
- (31) Senga, T.; Matsumi, Y.; Kawasaki, M. *J. Vac. Sci. Technol., B* **1996**, *14*, 3230.
- (32) Kaxiras, E.; Baryam, Y.; Joannopoulos, J. D.; Pandey, K. C. *Phys. Rev. B: Condens. Matter Mater. Phys.* **1987**, *35*, 9625.
- (33) Cometto, F. P.; Paredes-Olivera, P.; Macagno, V. A.; Patrino, E. M. *J. Phys. Chem. B* **2005**, *109*, 21737.
- (34) Hoft, R. C.; Gale, J. D.; Ford, M. J. *Mol. Simul.* **2006**, *32*, 595.
- (35) Gronbeck, H.; Curioni, A.; Andreoni, W. *J. Am. Chem. Soc.* **2000**, *122*, 3839.
- (36) Ohno, H.; Motomatsu, M.; Mizutani, W.; Tokumoto, H. *Jpn. J. Appl. Phys.* **1995**, *34*, 1381.
- (37) Redhead, P. A. *Vacuum* **1962**, *12*, 203.